Corrosion Engineering, Science and Technology

The International Journal of Corrosion Processes and Corrosion Control

ISSN: 1478-422X (Print) 1743-2782 (Online) Journal homepage: http://www.tandfonline.com/loi/ycst20

Impact specimen geometry on T23 and TP347HFG steels behaviour during steam oxidation at harsh conditions

T. Dudziak, M. Lukaszewicz, N. J. Simms & J. R. Nicholls

To cite this article: T. Dudziak, M. Lukaszewicz, N. J. Simms & J. R. Nicholls (2017) Impact specimen geometry on T23 and TP347HFG steels behaviour during steam oxidation at harsh conditions, Corrosion Engineering, Science and Technology, 52:1, 46-53, DOI: 10.1080/1478422X.2016.1185568

To link to this article: http://dx.doi.org/10.1080/1478422X.2016.1185568

Impact specimen geometry on T23 and TP347HFG steels behaviour during steam oxidation at harsh conditions

T. Dudziak*[1], M. Lukaszewicz[2], N. J. Simms[3] and J. R. Nicholls[3]

Ferritic T23 steel and austenitic TP347HFG steel have been studied with an emphasis on understanding the impact of specimen geometry on their steam oxidation behaviour. The selected materials were tested over a wide range of temperatures from 600 to 750°C. The tests were carried out in 100% steam conditions for 1000 hours. The tests indicated that the 'curved-shaped' specimens show slower mass gain, scale ticking and void nucleation rates than 'bridge-shaped' specimens (with flat and convex surfaces combined). Furthermore, a bridge TP347HFG sample showed the formation of lower amount of flaky oxide at 750°C.

Keywords: Steam oxidation, Steels, Energy sector, Shape, Ferritic, Austenitic, Oxidation

Introduction

Steam oxidation is matter of growing interest as research aimed at the improvement of power plant efficiency indicates the needs for higher temperatures and pressures. Each 1% increase in overall efficiency can result in as much as 3% reduction in CO_2 emissions.[1] Moreover, steam temperature in conventional power plants is expected to rise from 50 to 100°C by 2030 in order to reduce CO_2 emissions further. Currently, most of the coal-fired power plants operate at temperatures between 520 and 565°C and with pressures up to 180 bar achieving efficiencies of 38–40%.

In the new design units, the efficiency of energy generation is above 40% due to higher steam conditions (600–620°C). The most efficient power plants, currently designed and tested, are expected to have 44–46% efficiencies, with steam temperatures between 700 and 720°C and 360 bar pressure.

Using these operating conditions with traditional heat exchangers materials such as 16Mo3, 15HM, T22, T23 and other low-alloyed steels, the development of thick non-protective oxides is expected, resulting component failures.[2–4] Low-alloyed steels forming thick oxides resulting in concerns over tube overheating, scale spalling, tube blockages and steam turbine corrosion and erosion.[5] To mitigate these problems, constant research programmes have to be carried out to understand the influence of variety of factors such as steel composition, microstructure, time, temperature, operational conditions and finally the shape of the material.

[1]Foundry Research Institute, Centre for High Temperature Studies, Zakopiańska 73, 30-418 Krakow, Poland
[2]Exova (UK) Ltd, 12 High March, Daventry, Northamptonshire NN11 4HB, UK
[3]Cranfield University, School of Applied Science, Cranfield, Bedfordshire MK43 0AL, UK

*Corresponding author, email tomasz.dudziak@iod.krakow.pl

Owing to the severity of proposed operational conditions (temperatures and pressures) and the required lifetime at elevated temperatures, the materials used for the ultra-supercritical (USC) applications are required to exhibit very good mechanical, physical and chemical properties. Among these, oxidation and creep rapture resistance are believed to be of crucial importance. There are three groups of steels which could be successfully employed for the coal-fired boiler elements: ferritic, austenitic and nickel-based; however, their applications are limited up to 620 and 700°C, respectively. Owing to limited data on nickel-based steel there is no limit identified for their application, however it is proposed that for all applications above 700°C those materials should be used.[6]

High-temperature oxidation in 100% steam is characterised by faster oxidation rates than in dry or humid environments; moreover, the scale formed exhibits different adherence and porosity.[7] Both oxidation kinetics and the scale morphology are reported to be strongly dependent on the steel composition, surface finish and test conditions: metal temperature, steam flow and chemistry.[8]

Among highlighted factors, chromium levels are of crucial importance[9]; however, levels seems to have less impact below 570°C. Therefore for components operating at temperatures below 570°C the steels with lower Cr levels may be employed.[10] Viswanathan *et al.*[6] believes that chromium content has less impact on oxidation of 9–12% Cr ferritic steels below 600°C.

Nevertheless, there is no agreement on the impact of chromium on steam oxidation at different temperatures, but it is well recognised that steels with higher chromium level exhibit better oxidation resistance due to formation of more protective Cr rich oxides. However, there is no clear evidence for the minimum Cr content required for the development of the protective chromium oxides.

Shibli and Starr[11] indicated that in temperature range of 600–650°C, 10–11% of chromium in the base metal

Published by Taylor & Francis on behalf of the Institute
Received 3 March 2016; accepted 27 April 2016
DOI 10.1080/1478422X.2016.1185568

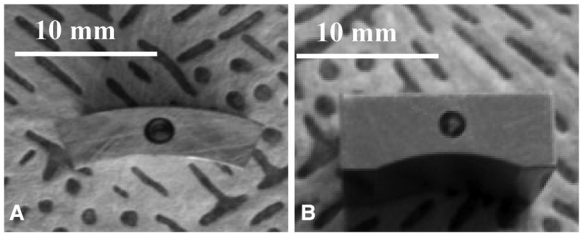

1 Specimen geometry: *a* curve shape, *b* bridge shape

allows protective, external chromia (Cr_2O_3) to be formed; in contrast Sanchez *et al.*[9] have shown that such an oxide forming with Cr content greater than 11–12% for steels exposed to steam at temperatures above 600°C. Quadakkers *et al.*[12] concluded that the scale formed on ferritic and austenitic steels differs with the chromium content in the base material; it is recognised that scale changes in following manner: with increasing Cr content it changes from haematite/magnetite to magnetite/(Fe, $Cr)_3O_4$ spinel to (Fe, $Cr)_3O_4$ spinel/Cr_2O_3 and finally to a pure Cr_2O_3.

Viswanathan *et al.*[6] proposed the following ranking of the high-temperature resistant steels, due to their chromium levels and their relation with protective properties of the scale: IN740, Haynes 230, HR120, HR6W, HR3C, TP347HFG, Super 304H, T92, T91 and finally T23.

The scales formed on the high-temperature resistant steels differ with alloy type; this is clearly associated with the chromium level as presented above, additionally the alloy structure and grain size are reported to have considerable impact.[4] Oxides developed on the ferritic steels have a duplex structure,[7] an inner layer with protective chromium oxides and an outer with magnetite as the main constituent.[6] Although expected, the continuous layer of haematite is not always present as the outermost layer. Often there are traces of Fe_2O_3 on the surface of magnetite however it is discontinuous. Haematite is believed to form due to reduced iron diffusion through the magnetite.

The slower diffusion is result of the gap nucleation between inner and outer layers or within the outer Fe_3O_4. The double-layered scale was also found on the austenitic steels, with (Fe, Cr) spinel (inner layer) and magnetite (outer layer) as the main constituents,[6] however such scale forms after long-term exposure. Viswanathan *et al.*[5] and Hansson and Montgomery[4] indicated that scale formed on the austenitic alloys changes with temperature; below 585°C it shows irregular structure with some porosity, above that temperature the scale seems to be more homogenous.[4] To summarise, the main difference between the scales formed on the ferritic and austenitic steels are their properties – uniformity, thickness, porosity and adherence.[2,3,13]

Because the impact of temperature and chemical composition is well known from past research,[1–24] here, particular attention was paid to the impact of the steel shapes, on steam oxidation resistance in temperature range 600–750°C for 1000 hours. This was done using low-alloyed ferritic steel T23 and medium alloyed austenitic TP347HFG steel.

Experimental

Materials

The materials selected for steam oxidation experiments were represented by two steels with different chemical compositions and different high-temperature behaviour. The T23 and TP347HFG steels in the form of a curve (15 mm × 15 mm) and bridge (15 mm × 15 mm) shape specimens were machined and are presented in Figs. 1 and 2 correspondingly.

The wall thickness was 3 mm for TP347HFG and 5 mm for T23, respectively. Before the exposure, the samples were ground to a 600 grit surface finish and cleaned in volasil. Subsequent to this step, isopropanol in ultrasonic bath for 10 minutes was used. The nominal chemical composition of the tested materials is summarised in Table 1.

Steam oxidation test

Steam oxidation tests were carried out in a horizontal tube furnace equipped with an alumina lined reaction tube equipped with stainless steels flanches (Fig. 3). The samples were exposed to a 100% steam environment for four cycles, each 250 hours giving 1000 hours of exposure per test. The steam flow rate was set up for 12 l/h which equals a velocity of 3.6, 3.8, 3.9 and 4.1 mm s^{-1} at 600, 650, 700 and 750°C, respectively. The specimens were placed in alumina crucibles to enable an overall mass

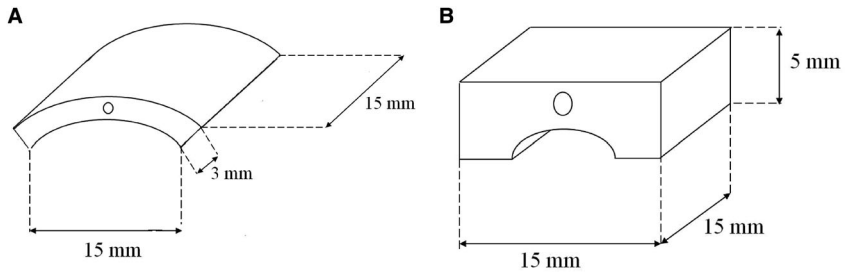

2 Test samples drawing: *a* curve shape, *b* bridge shape

Table 1 Composition of the investigated alloys (wt-%)

Alloy	C	Ni	Cr	Mo	W	Co	Mn	Fe	Si
T23	0.06	…	2.25	1.00	1.50	…	0.45	Bal.	0.20
TP347HFG	0.10	10.00	18.00	…	…	…	1.60	Bal.	0.60

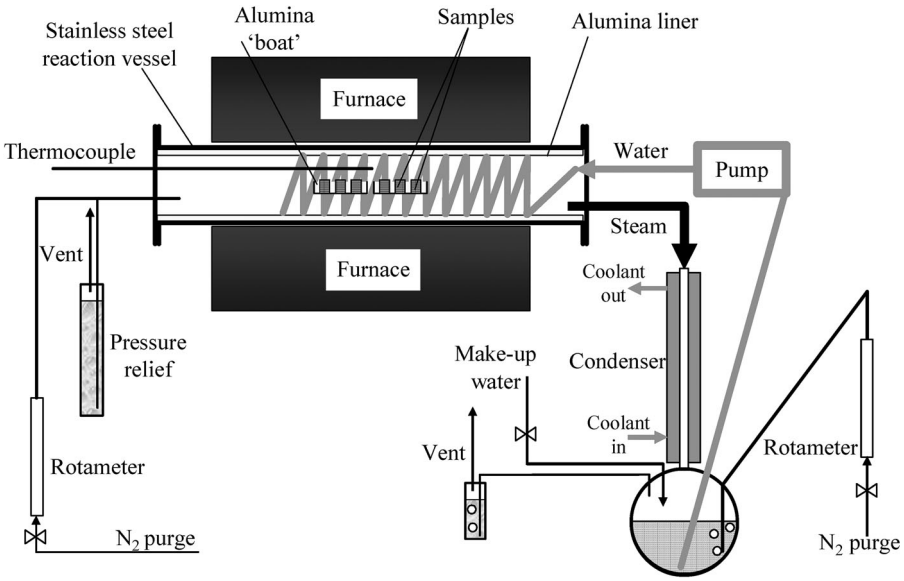

3 Schematic diagram of the steam oxidation tests facility

change analysis (including spallation) and ensure a proper data assessment.

In a steam oxidation test facility, steam was generated by pumping deionised water from a reservoir into the furnace before being passed over the tested samples and flown back into a condenser before reaching the reservoir. The water used in the reservoir was double de-ionised. Before starting the test facility, the system was sealed and thoroughly purged using 'oxygen free nitrogen'.

This purge continues through the water reservoir throughout the samples exposure period to minimise the level of oxygen in the system. The individual crucibles with the samples were placed in the furnace hot zone (calibrated before the experiment) and heated in a nitrogen atmosphere to 100°C.

Once this temperature was reached, the nitrogen gas supply was turned off and the furnace temperature was ramped up to the required temperature, meanwhile, a peristaltic pump was turned on in order to deliver water into the hot zone of the furnace. During the tests, hot steam was passed around the exposed samples and reaching the end of the Al_2O_3 liner in order to condensate and return to the reservoir. The exposed samples were cooled down to room temperature in a 100% nitrogen atmosphere by switching off the power supply after every 250 hours.

After 1000 hours, the exposed steel samples were examined using Environmental Scanning Electron Microscopy (ESEM) (Philips XL 30) in Back Scatter (BSE) mode, coupled with an Energy Dispersive X-ray (EDX) analyser (Oxford INCA). Phase development upon steam oxidation was investigated using an X-Ray Diffractometer (Siemens 5005) using radiation angles between 10° and 90°. Kinetics of the exposed specimens was weighed using a highly accurate analytical Sartorius CP323P balance.

Results

Kinetics

The steam oxidation experiments were carried out between: 600, 650, 700 and finally 750°C. Figures 4 and 5 show the mass change for T23 and TP347HFG steels after a 1000 hour exposure t in a steam environment, respectively. In addition, Figs. 4 and 5 demonstrate the differences in mass change associated with the shape of the exposed sample.

It was found that mass change of each steel type varies with the sample shape. Figure 6 shows the distribution of the mass change results for ferritic steel T23 at all analysed temperatures; the curves show that weight gain varies with a specimens' geometry. The bridge shapes samples show a larger mass change between 600 and 700°C. At 750°C, after 1000 hours exposure, the curve shaped specimen demonstrated a larger mass change.

Figure 7 demonstrates that TP347HFG steel exhibited even larger differences in mass gain as a function of shape. TP347HFG steel exposed at 600, 700 and 750°C, indicates a faster mass change for the bridge shape samples. However, at 650°C the curved sample shows a faster mass gain. Moreover, the curved specimens show similar mass changes at 650 and 750°C. In the case of bridge samples, the mass changes significantly with temperature from 0.05 to 0.4 mg cm^{-2} at 650 and 750°C, respectively. At 700°C, samples indicate the largest mass gain, which do not vary with sample geometries.

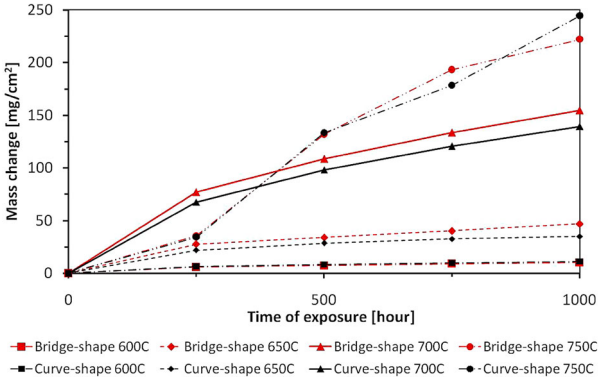

4 Comparison of mass change data for T23 steel between 600 and 750°C (overall mass change including spallation)

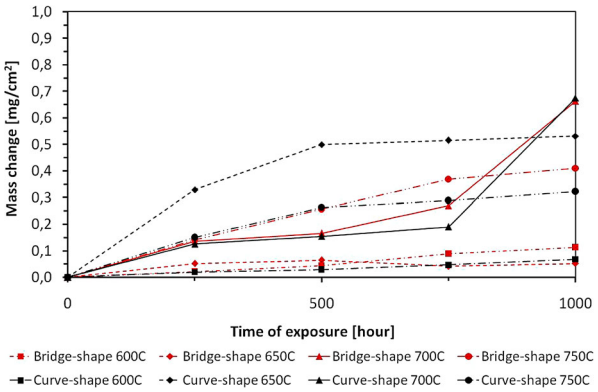

5 Comparison of mass change for TP347HFG steel between 600 and 750°C (overall mass change including spallation)

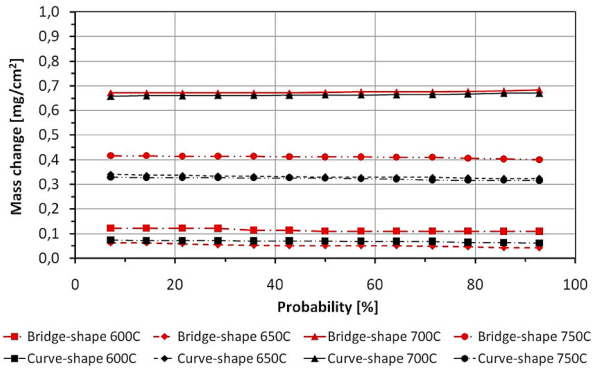

7 Distribution of mass change result for TP347HFG steel after 1000 hours exposure between 600 and 750°C (overall mass change including spallation)

Surface microstructures

The microstructures of the oxide scales developed on the steels vary with temperature, specimen geometry and chromium concentration. Figure 8*a*, *c*, *e* and *g*, and *b*, *d*, *f* and *h* shows the surface microstructures of T23 and TP347HFG steels with bridged and curved shapes, respectively. Owing to the fact that morphologically bridge and curve shaped samples show a similar phase formation, in this section, bridge-shaped samples will be disused.

The surface of T23 steel at tested temperatures was covered with a mixture of iron oxides. At 600°C, the top layer consisted of haematite (Fe_2O_3) on both curved and bridge-shaped specimens; some magnetite (Fe_3O_4) rich areas were also found, however this oxide was identified beneath the haematite layer as shown in Fig. 8a. With increasing temperature the amount of haematite decreased, at 750°C a lack Fe_2O_3 was found. Furthermore, the scale formed at 600 and 650°C starts to exfoliate on the T23 ferritic steel due to the surface cracking through the outer oxide layers (Fig. 8a and g). In comparison at 700 and 750°C oxides layers are fully adherent to the surface, there is minimal exfoliation and surface cracking observed (Fig. 8e and g).

The chemical composition of the surface, examined by EDX has been compared with phase analyses carried out with XRD. The results from both investigations showed good agreement, confirming the formation of haematite (Fe_2O_3) and magnetite (Fe_3O_4) in T23 steel. The phases constituents were evaluated based on EDX analyses, where Fe_2O_3 was comprised of around 70 wt-% Fe, Fe_3O_4 72 wt-% Fe and FeO possessed around 80 wt-% Fe.

The bridge and curve shaped TP347HFG steels developed thin layer of the protective oxide at lower temperatures (600 and 650°C). This layer consisted of a Mn–Fe–Cr–O mixture with a composition of 9.5–14.6–45.1–29.3 wt-%, respectively. The XRD investigations performed on the exposed steels demonstrated that phases such as $MnFe_2O_3$ and $Cr_{1.3}Fe_{0.7}O_3$ were present, confirming elementary findings at the surface. At higher temperatures (700 and 750°C), the steel TP347HFG was covered with a thin oxide scale with a similar composition to those shown at 600 and 650°C. At the temperatures of 600 and 650°C, the diffusion rate in TP347HFG is rather low,

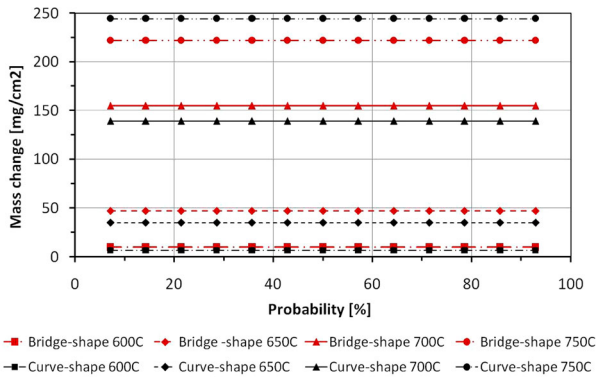

6 Distribution of mass change result for T23 steel after 1000 hours exposure between 600 and 750°C (overall mass change including spallation)

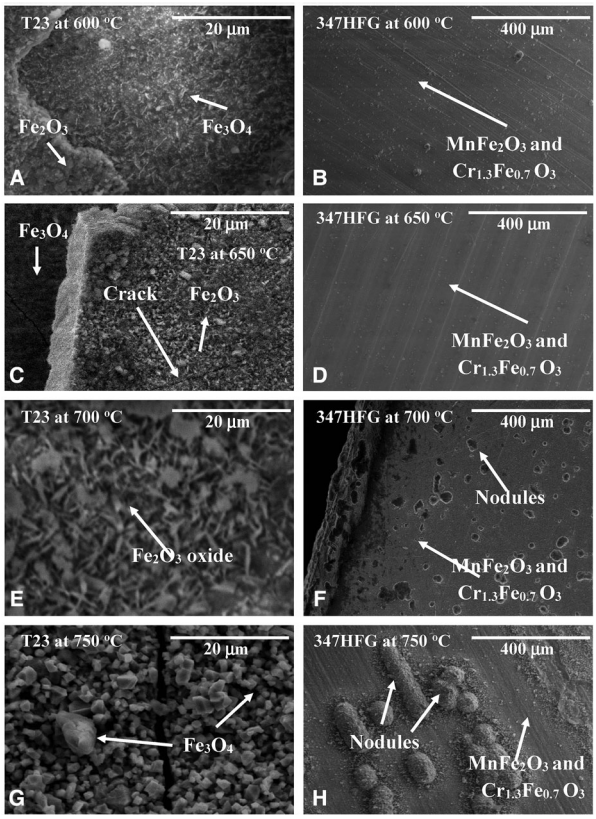

8 Surface microstructures of oxidised bridge shape surfaces after 1000 hours exposure at elevated temperatures

therefore formation of the scale rich in Cr is expected due to fine grain structure. Such structures offer a higher grain boundary area and thus promote grain boundary diffusion. Owing to a higher content of Cr and fine grain structure, it is beneficial to develop a protective chromium oxide layer under steam oxidation conditions; however, this protectiveness, as shown in this work is limited. Based on the SEM micrographs and associated EDX data, it was found that the steel underwent accelerated degradation throughout nodule formation. It was found that with increasing temperature, the number of nodules increased (Fig. 8f and h). Nodule formation developed due to local imperilment of the protective oxide and outward diffusion of Fe.

Cross-sectional microstructures

Figure 9a–h shows cross-sectional images performed by SEM in BSE mode. At a temperature of 600°C (Fig. 9a and b), both bridged and curved samples show three distinguishable oxide layers. The innermost layer was occupied by a mixed chromium and iron oxide spinel type structure $(Fe,Cr)_2O_4$ with a low Cr concentration (5 wt-%) and 1–2 wt-% W, whereas the Fe_3O_4 phase occupied the middle layer. Finally, the top part of the oxide scale was consisted of Fe_2O_3.

The phases constituents were evaluated based on EDX analyses, where Fe_2O_3 consisted of around 70 wt-% Fe, Fe_3O_4 72 wt-% Fe and FeO possessed around 80 wt-% Fe. The innermost layer was adherent to the metal matrix for both curved and bridge-shaped specimens.

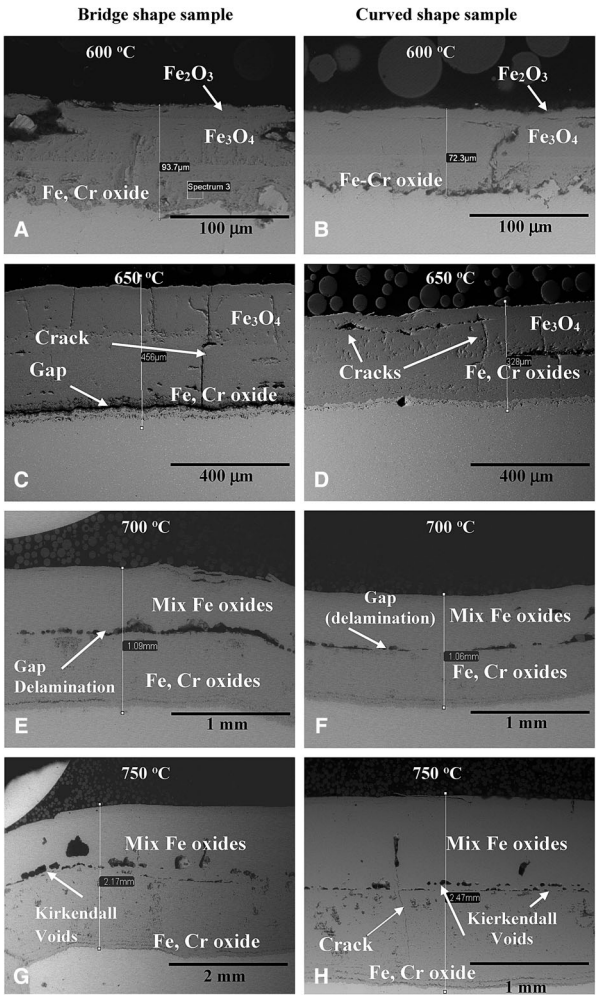

9 Cross-section microstructures developed on the T23 bridge and curved shaped samples; after 1000 hours

In contrast, at slightly higher temperatures (650°C), the curved shape samples lost adherence due to gap development at the substrate – oxide scale interface (Fig. 9c) and crack formation within the oxide scale was observed (Fig. 9d). The delaminated part of the scale showed higher iron levels than the inner part of the scale, therefore the conclusion is that its main constituents are Fe_2O_3 and Fe_3O_4. In case of the curve shaped samples, there are no gaps and the scale maintains the adherence for the entire test period, however, it develops more cracks within the layer and there are a significant number of voids, which eventually will coalesce and, finally, due to the stress generated within the scale, it will lose its adherence and exfoliate.

Steam oxidation of T23 steel at 700 and 750°C (Fig. 9g and h) caused the development of thicker scale than that observed at lower temperatures. The scale was observed to be multilayered with lack of protectiveness but good adherence was formed. Chemical analyses identified throughout EDX showed the formation of a mix of iron oxides, with Cr distribution within the layers differing substantially. Cr was found only at the oxide scale – substrate interface showing the formation of an iron oxide spinel type structure $(Fe,Cr)_2O_4$ with Cr concentration (10 wt-%) and 2–4 wt-% W. Furthermore, it was found that a large void formed within the oxide scale (Fig. 9h), which initiated crack formation towards the substrate throughout the innermost layer in the curved shape sample. In the bridge-shaped sample, such phenomena was not indicated.

The outer layer was occupied by the formation of Fe_3O_4. In the case of the T23 steel, there is no outermost layer of haematite present when exposed at lower temperatures. At the interface between the inner and outer layers, voids have coalesced for both curved and bridged samples. The oxide scale developed on curved specimens was thicker than that on the flat part of the bridge shape, whereas on the concave surface the oxides seem to be thicker and exhibit higher porosity (gaps, Kirkendall voids).

Similar observations have been conducted by Tuck *et al.*[14] where pure iron and low-alloyed steels have been investigated. The observed porosity on the exposed sample has been related to the geometry of the specimen. The investigation has showed compact scales with no porosity on flat surfaces, however, porous scales were formed on curved surfaces. In this study, next to the metal oxide interface, the grain boundaries start to be visible due to voids injections. This was not observed in case of the curved specimens.

In comparison, steam oxidation of austenitic TP347HFG steel led to the formation of much thinner and much more protective oxide scales than those observed on T23 steel (Fig. 10a–f). This is due to a much higher Cr content in the metal matrix, however, as mentioned previously, high-temperature protectiveness is limited due to nodule formation found on the surface.

In contrast to the T23 steel, the shape of the exposed sample showed a lack of influence on the oxide scale adhesion. In both bridged and curved shaped TP347HFG samples, similar phases formed. The oxide nodules have been observed after 1000 hours exposure at 700 and 750°C and showed a two layered structure (Fig. 10d and f). The outer layer was rich in iron with a

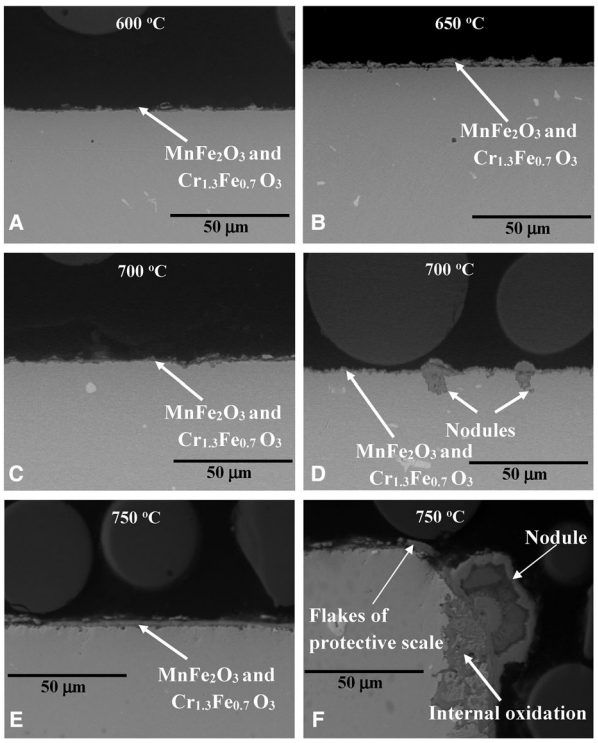

10 Cross-section microstructures of 347HFG steel exposed at elevated temperatures showing different rate of degradation

small quantity of Cr, the inner layer consisted mixture of Cr, Ni and Fe oxides and underneath the nodule formation a large area of internal oxidation was formed.

TP347HFG steel was covered with a more protective mixture of chromium, iron oxide $Cr_{1.3}Fe_{0.7}O_3$ and $MnFe_2O_3$, the thickness of the formed oxide differs with the exposure time and temperature, however this dependence is less visible than that observed in ferritic steel T23. Furthermore at the highest temperature (750°C), adhesion of the oxide scale decreased in TP347HFG steel, showing some flake formation. A higher number of flakes were found in curved shape samples in comparison with bridge-shaped samples.

Discussion

Oxidation of T23 at investigated temperatures seems to follow the parabolic law at 600–650°C, however above 650°C the process significantly accelerates. This is most probably due to the FeO formation where, after longer exposure it could transform to linear. This is in accordance with Wright and Pint,[15] who concluded that at temperatures above 600–650°C, the steam oxidation rate is closer to linear. It was also confirmed by Lepingle *et al.*[16] that the oxidation of T23 starts to exhibit dependence close to linear above 650°C. Results of the tests in this study show that steam oxidation in a temperature range 600–750°C shows parabolic rate dependence (750°C) and the oxidation rate follows. At 600°C, the oxidation of T23 is much slower; Komai *et al.*[17] and Lepingle *et al.*[16] believed that it followed parabolic behaviour.

The activation energy for T23 at analysed temperatures was calculated to be −335 kJ mol^{-1} which is in good agreement with Fry *et al.*[18] In contrast, Wright and Dooley[19] have calculated the activation energy in the temperature range between 500 and 700°C as being −230 kJ mol^{-1}, however that value was based on the number of independent tests performed by different groups of researchers. The discrepancy in results is most probably caused due to diverse test conditions, experimental procedures and the analytical approaches to the data obtained. According to Paterson *et al.*[20] a change in steam pressure results in a thicker scale formation, which means that the oxidation rates are faster and therefore the values of the activation energy differ. There are number of the variables such as steam flow and water chemistry which may also influence the results.[8]

The tests conducted showed a slower oxidation rate for TP347HFG steel at the temperatures of interest. This rate his is associated with its higher chromium content and therefore formation of more protective oxides which significantly slow down the oxidation process.[5] There is only a limited number published studies on the oxidation kinetics of TP347HFG at high temperatures in steam at 1 bar.[5] Wright and Dooley[19] show that even after a longer exposure to high temperatures, the TP347HFG shows a slower oxidation rate. Moreover, the work of Hansson and Montgomery[4] confirmed oxidation of this type of steel to be slow; with the oxide scale of TP347HFG exposed at 625°C after over 7000 hours being still less than 1 μm thick, corresponding with slow oxidation rates. Analysis of the oxidation kinetics of TP347HFG shows that oxide growth rates do not fully follow the parabolic rate law, therefore it is assumed to be sub-parabolic.

In contrast, Wright and Dooley[19] believed that the oxidation of the TP347HFG at high temperature closely follows the parabolic rate law. This is also in agreement with Viswanathan *et al.*[5] and Saunders and McCartney.[21] Activation energies derived from the data obtained in this study are in agreement with Fry *et al.*[1,8] who give an energy value of-132 kJ mol^{-1}. The differences in activation energies values are most probably due to different sample treatments, exposure conditions and procedures.[8]

As presented in the results section, the scale developed on T23 at 600 and 650°C was double-layered with local growth of a third outermost layer of haematite, showing agreement with Otsuka[10] and Nishimura *et al.*[22] Moreover Lepingle *et al.*[16] and Komai *et al.*[17] indicated that the scale consisted of two types of oxides; the inner layer is rich in the $(Fe,Cr)_3O_4$ spinel, whereas the main constituent of the outer layer is magnetite. Additionally, there are some traces of the haematite identified as the outermost layer.[5,19]

In particular tests, the haematite has formed between 600 and 700°C; there is no trace of it at 750°C. Fe_2O_3 forms on the surface of T23 samples at the beginning of the process most probably due to the relatively high oxygen partial pressure, as the result of the slower iron diffusion from the metal to the magnetite, which is caused by the existence of the Cr rich spinel.[17] After longer exposure, when the protective properties of the Fe–Cr spinel are lower due to fact that T23 steel is not able to sustain the protective layer (low Cr content in the base material), haematite forms above the region with large amount of voids and cracks significantly reducing the iron diffusion.[22] At higher temperatures (700–750°C), a multilayered inner scale forms. According to Wright and Dooley,[19] this structure consists of the repeating double series of the Fe–Cr spinel, however EDX analysis shows

a significant content of the iron corresponds with magnetite, therefore the conclusion is that the multilayered structure is mix of the Fe–Cr spinel and Fe_3O_4.

Some authors report a multilayered inner structure forming as a result of heat flux,[19] the heat flux is reported by Osgerby and Quadakkers[8] to be the major difference between laboratory exposure procedures and plant conditions. Griess *et al.*[23] have shown that even at higher temperatures, in laboratory tests the oxidation rates and scale changes are slower than in exposures where the heat flux is present. However the existence of multilayered oxides may be explained by higher exposure temperatures. Under such conditions, wustite (FeO) is able to form, when the scale cools down the wustite layer decomposes to magnetite and in many cases transforms to duplex layer of magnetite or mixed Fe_3O_4 and Fe–Cr spinel. A multilayered inner structure is explained as a result of steam flow rates causing faster oxide growth.

The double-layered oxide scale is present in both types of the specimen geometries; however, its thickness differs. The oxides developed on the bridge-shaped specimens are thicker for both 600 and 650°C. The scale is the thickest on the concave and flat surfaces of the specimen. It is thinner where the flat surface transforms to become concave. This is associated with stress development which causes scale exfoliation; the scale growing there will be under higher stress, therefore there is greater probability of scale spallation. Additionally, at temperature of 650°C, there is substantial amount of haematite growing on that part of the scale, which will again lead to exfoliation due to differences in the coefficients of thermal expansion between Fe_2O_3 and Fe_3O_4.[12]

The stress generated upon sample cooling is tensile, moreover according to Otsuka[10] the exfoliation is affected by the radial stress, which leads to spallation if it is larger than the adhesion strength of the oxide scale. During the exposure of bridge samples, the gaps nucleate at the inner/outer scale interface, within the oxides at the concave surface and at the transition between the flat and concave surfaces; however, they heal after longer exposure times. The healing may be explained by access of oxygen molecules through magnetite and haematite[12]; instead there is gap between metal and oxide scale. On the other hand, there are more voids a with a gap present at the interface between inner and outer scale of the curved samples which results in the haematite formation.[22] The amount of haematite on the surface of the analysed samples was also dependent on the sample position within the furnace. The part of the samples facing the steam flow develops more Fe_2O_3 due to the higher partial pressure of O, later partial pressure of O decreased for Fe – oxide formation, thus a slightly lower amount of haematite was found on the other samples placed further from steam flow.

Furthermore, the amount of haematite is larger on the curve and the concave part of the bridge-shaped specimens, where voids and gaps have formed. In contrast, the surface which is at the counter-position to steam flow shows less haematite and spallation.

The scales formed on the TP347HFG analysed are significantly thinner than those on T23; this is result of the formation of a protective oxide.[15] According to the Viswanathan *et al.*,[5] the scale formed on austenitic steels is 2–3 times thinner than on ferritics; however, for these particular tests the difference is more significant. The better resistance of the TP347HFG is not just associated with higher chromium content (18 wt-%) but also with the grain structure.[4,19] The fine grain structure of TP347HFG significantly increases the Cr supply to the protective oxides by grain boundary diffusion and so the thin chromia scale can lasts longer. Hansson and Montgomery[4] reported that even after over 7000 hours exposure at 625°C the steel is covered with thin (~1 μm) layer of Cr_2O_3. Additionally, they show that a uniform layer of chromia is able to form after 500 hours at 700°C and suppresses the un-protective oxide growth up to 2000 hours. For particular tests, a thin layer of $Cr_{1.3}$, $Fe_{0.7}O_3$ and $MnFe_2O_4$ has formed after exposure at all temperatures tested, however its thickness varies with exposure conditions. The fast development of the protective oxides scale above 700°C is due to *enhanced* chromium diffusion in the grain boundaries.[4] After longer exposure at 700 and 750°C, the protective scale breaks down and double-layered nodules start to nucleate on the surface. The protective oxide scale formed on TP347HFG is able to prevent fast nodular growth; however, eventually after longer exposures, the double-layered scale will spread along the surface.[19] The double-layered nodule consists of iron oxide with some traces of chromium and nickel, whereas the inner part is a mix of Fe–Cr spinel and magnetite. The formation of the nodules is explained by the penetration of the protective scale along the grain boundaries. Furthermore, due to the outward diffusion of chromium, the chromium-depleted boundaries are able to oxidise to magnetite. Moreover, development of the nodular oxides is influenced by surface defects, additionally the number of nodules increases in the corners and on the edges of the samples, which is associated with grain orientation and higher stresses within the material.

Following longer exposure, the surfaces of TP347HFG forms a double-layered scale, which at temperatures between 575 and 650°C and steam at 1 bar consists of an outer layer with magnetite as the main constituent and the inner structure of Fe–Cr spinel.[19] This is in agreement with findings from Hansson and Montgomery.[4] However, Ughes *et al.*[24] have shown that at 670°C after 11 000 hours a double layer forms, where the outer layer is mix of Fe_2O_3 and Fe_3O_4 whereas the inner layer consists of Cr_2O_3.

Conclusions

Steam oxidation performance of the T23 and TP347HFG steels at 600, 650, 700 and 700°C with special consideration of the specimen geometry were analysed and discussed. Based on obtained results from 1000 hours tests the following conclusions are drawn:

1. T23 (2.25 wt-% of Cr) steel shows a much thicker oxide development at each of tested temperatures, a thick oxide formed due to low Cr concentration in the substrate.
2. The formation of a three-layered oxide structure consisting Fe_2O_3, Fe_3O_4, a mixture of Fe and up to 15 wt-% Cr with a tiny W content has been found in T23 ferritic steel.
3. There is a clear impact of the specimen geometry on the mass change of the T23 sample based on Figs. 4 and 5.
4. The samples with more complex geometries indicated larger mass changes based on findings on Figs. 4 and 5.

5. The curved shape specimens had an oxide scale which was thicker than that observed on the flat part of the bridge shape, whereas on the concave surface the oxides seem to be thicker and exhibit higher porosity (gaps, Kirkendall voids).
6. At the interface between inner and outer layers, voids have coalesced for both curved and bridge samples.
7. The formation of Kirkendall voids in T23 steel at the interface between inner layers has been observed at 750°C.
8. The formation of nodules at 700 and a higher number at 750°C have been observed in curved and bridge shape samples suggesting similar behaviour and limited oxidation resistance during longer exposures.
9. Under steam oxidation conditions, the TP347HFG austenitic steel developed microstructure consisting of $MnFe_2O_3$ and $Cr_{1.3}Fe_{0.7}O_3$ in temperature range of 600–750°C.

Acknowledgements

We would like to acknowledge the support of The Energy Programme, which is a Research Councils UK cross council initiative led by EPSRC and contributed to by ESRC, NERC, BBSRC and STFC, and specifically the Supergen initiative (Grants GRyS86334y01 and EPyF029748) and the following companies; Alstom Power Ltd., Doosan Babcock, E.ON, National Physical Laboratory, Praxair Surface Technologies Ltd, QinetiQ, Rolls-Royce plc, RWE npower, Siemens Industrial Turbomachinery Ltd. and Tata Steel, for their valuable contributions to the project.

References

1. J. Henry, G. Zhou and T. Ward: 'Lessons from the past: materials-related issues in an ultra-supercritical boiler at eddystone plant', *Mater. High Temp.*, 2007, **24**, 249–258.
2. P. J. Ennis and W. J. Quadakkers: 'Implications of steam oxidation for service life of the high-strength martensitic steel components in high-temperature plant', *Int. J. Pres. Ves. Pip.*, 2007, **84**, (1-2), 82–87.
3. P. J. Ennis and W. J. Quadakkers: 'Mechanisms of steam oxidation in high strength martensitic steels', *Int. J. Pres. Ves. Pip.*, 2007, **84**, (1-2), 75–81.
4. A. N. Hansson and M. Montgomery: 'Long term steam oxidation of TP347H FG in power plant', *Mater. High Temp.*, 2005, **22**, (3-4), 263–267.
5. R. Viswanathan, J. Sarver and J. M. Tanzosh: 'Boiler materials for ultra supercritical coal power plants – steamside oxidation', *J. Mater. Eng. Perform.*, 2006, **15**, (3), 255–274.
6. R. Viswanathan, R. Purgert and U. Rao: Materials technology for advance coal power plants EPRI Report, 2002.
7. J. Gabrel, C. Coussement, L. Verelst, R. Blum, Q. Chen and C. Testani: 'Superheater materials testing for USC boilers: steam side oxidation rate of advanced materials in industrial conditions', *Mater. Sci. Forum.*, 2001, **369–372**, 931–938.
8. S. Osgerby and J. Quadakkers: 'The influence of laboratory test procedures on scale growth kinetics and microstructure during steam oxidation testing', *Mater. High Temp.*, 2005, **22**, 27–33.
9. L. Sanchez, M. P. Hierro and F. J. Perez: 'Effect of chromium content on the oxidation behaviour of ferritic steels for applications in steam atmospheres at high temperatures', *Oxid. Met.*, 2009, **71**, (3-4), 173–186.
10. N. Otsuka: 'Fracture behavior of steam-grown oxide scales formed on 2–12%Cr steels', *Mater. High Temp.*, 2005, **22**, (1-2), 131.
11. A. Shibli and F. Starr: 'Development of and integrity issues with new high temperature high strength steels', *Int. J. Pres. Ves. Pip.*, 2007, **84**, (1-2), 114–122.
12. W. Quadakkers, P. Ennis, J. żurek and M. Michalik: 'Steam oxidation of ferritic steels – laboratory test kinetic data –,workshop on scale growth and exfoliation in steam plant', *Mater. High Temp.*, 2007, **22**, (1-2), 47–60.
13. J. Ehlers, D. J. Young, E. J. Smaardijk, A. K. Tyagi, H. J. Penkalla, L. Singheiser and W. J. Quadakkers: 'Enhanced oxidation of the 9% Cr steel P91 in water vapour containing environments', *Corros. Sci.*, 2006, **48**, (11), 3428–3454.
14. C. W Tuck, M. Odgers and K. Sachs: 'The oxidation of iron at 950°C in oxygen/water vapour mixtures', *Corros. Sci.*, 1969, **9**, 271–285.
15. I. G. Wright and B. A. Pint: An assessment of the high-temperature oxidation behaviour of Fe–Cr steels in water vapour and steam Denver, USA NACE Corrosion, 2002.
16. V. Lepingle, G. Louis, D. Petelot, B. Lefebvre and J. Vaillant: 'High temperature corrosion behaviour of some boiler steels in pure water vapour', *Mater. Sci. Forum.*, 2001, **369–372**, 239–246.
17. N. Komai, F. Masuyama and M. Igarashi: '10-year experience with T23 and T22 in a power boiler', *J. Press. Vessel. Technol.*, 2005, **127**, (2), 190–196.
18. A. Fry, S. Osgerby and M. Wright: 'Oxidation of alloys in steam environments – a review', 2002, UK, National Physical Laboratory (NPL).
19. I. G. Wright and R. B. Dooley: 'A review of the oxidation behaviour of structural alloys in steam', *Int. Mater. Rev.*, 2010, **55**, (3), 129–167.
20. S. R. Paterson, R. Moser and T. Rettig: Electric Power Research Institute/VGB Technische Vereinigung der Grosskraftwerksbetreiber in Atomic Energy Commission USA -Reports-; 8-1; Interaction of iron-based materials with water and steam by EPRI; 1993.
21. S. R. J. Saunders and L. N. McCartney: 'Current understanding of steam oxidation - power plant and laboratory experience', *Mater. Sci. Forum.*, 2006, **522–523**, 119–128.
22. N. Nishimura, N. Komai, Y. Hirayama and F. Masuyama: 'Japanese experience with steam oxidation of advanced heat-resistant steel tubes in power boilers', *Mater. High Temp.*, 2005, **22**, 3–10.
23. J. C. Griess, J. H. DeVan and W. A. Maxwell: Long-term corrosion of Cr–Ni steels in superheated steam at 482 and 538°C, NACE Corrosion 81, April (Toronto, Canada), NACE, Houston, TX, 1981.
24. A. H. Ughes, R. B. Dooley and S. Paterson: Oxide exfoliation of TP347HFG in high-temperature boilers, Institute of Materials Engineering Ltd, Australia, Sydney, 2003.